Investigating the removal of particles from the air/water-interface – Modelling detachment forces using an energetic approach

Knüpfer, P.; Fritzsche, J.; Leistner, T.; Rudolph, M.; Peuker, U. A.;

Originally published:

October 2016

Colloids and Surfaces A: Physicochemical and Engineering Aspects 513(2017), 215-222

DOI: https://doi.org/10.1016/j.colsurfa.2016.10.046

Perma-Link to Publication Repository of HZDR:

https://www.hzdr.de/publications/Publ-24047

Investigating the removal of particles from the air/water-interface – Modelling detachment forces using an energetic approach

Paul Knüpfer[1]*, Jörg Fritzsche[1a], Tom Leistner[2b], Martin Rudolph[2c] and Urs Alexander Peuker[1d]

[1]*Institute of Mechanical Process Engineering and Mineral Processing, Agricolastraße 1, 09599 Freiberg, Germany*

[2]*Helmholtz-Zentrum Dresden Rossendorf, Helmholtz Institute Freiberg for Resource Technology, Chemnitzer Str. 40, 09599 Freiberg, Germany*

*corresponding author: paul.knuepfer@mvtat.tu-freiberg.de

[a]joerg.fritzsche@mvtat.tu-freiberg.de

[b]t.leistner@hzdr.de

[c]m.rudolph@hzdr.de

[d]urs.peuker@mvtat.tu-freiberg.de

Abstract

For solid particles it is energetically favorable being situated at the interface of fluid phases and removing a particle from an interface requires a high force. The capillary force affects at the particle and causes an interfacial deformation during detachment. In this study the detachment force of hydrophilic and hydrophobic particles is measured via CP-AFM. In order to calculate the detachment force, a simple analytical model is developed and compared with the classical capillary force model. The new model is grounded on an energetic approach in compliance to the interfacial deformation and wetting of the particle. A model spring is assumed for both sub-processes and the force affects onto these two springs. The calculated force in the new model referred to goes better with experimental values than the capillary force model which does not consider interfacial deformation.

Research highlights

- CP-AFM measurements of the detachment force of colloidal particles from liquid interfaces
- Spring model for calculating the detachment force by respecting interfacial deformation
- Comparing the measured and calculated forces with the capillary force model

Abbreviations

AFM, Atomic Force Microscopy; A-AW, air to air-water-interface; TPC, three phase contact; W-WA, water to water-air-interface;

Keywords: AFM; capillary force; detachment force; energy of adhesion; interfacial deformation; spring model

1. Introduction

Interfacial processes play a key role in many industrial processes. Especially the attachment and detachment of particles at fluid interfaces strongly effect the overall performance of processes like agglomeration [1], froth flotation [2] and filtration [3]. Froth flotation uses the selective attachment of hydrophobized particles to the gas-liquid-interface of the bubble. Agglomeration applies liquid-bridges between solid surfaces to generate high attractive forces. Interaction forces e.g. control the adhesion of particles at the filter surface of deep bed filters. In the case of deep bed filtration of metal melts for instance, the collection of non-wetted particles in porous ceramic foam filters is increased if the filter surface has the same surface properties. The higher the welling angle, the surface energy respectively, of the solid surfaces becomes, the higher is the probability for the presence of nano-bubbles [4]. The latter create attractive gas bridges, which lead to agglomeration of dispersed particles [5] or the collection of dispersed particles onto the inner filter surface [3]. Capillary interactions are also important in the flotation process and have as well been studied with colloidal probe atomic force microscopy [6,7].

From a thermodynamic point of view, for particles it is energetically favorable being placed at the interface of two fluid phases. Compared to molecular surface-active substances like surfactants the adsorption of particles is not a reversible process. Therefore the adsorption of particles cannot be described as adsorption equilibrium for small particles. That is due to the magnitude of the energy of adhesion, which is much larger than the thermally induced kinetic energy $k \cdot T$ [8,9]. Thus once a particle is trapped in an interface, it is difficult to remove it from there.

Many authors have measured and reported capillary forces acting on microspheres, which are in contact with a fluid interface, either if the particle has been moved from the gas phase (air) into an air-water interface (drop, system A-AW) [10–12] or in the opposite direction from a water phase into a water-air interface (bubble, system W-WA) [10,12–19]. Also investigations using particles with sharp edges can be found in literature [20]. All these measurements provide knowledge considering the behavior of particles at fluid interfaces, the forces acting on the particle during attachment and detachment and the surface properties of the particle. Numerical models for calculating the process are reported as well [21,22]. In this paper, we report on the measurements of the capillary forces between hydrophilic and hydrophobic particles, respectively, and fluid interfaces. Furthermore, a simple spring model, based on energetic considerations, is presented to calculate these forces. This model describes the physics of the process much better than the simple capillary models used so far. Finally, a comparison between measured and modelled forces is given.

2. Materials and Methods

An atomic force microscope (AFM) XE-100 from Park Systems is used throughout this investigation. An external data recording system, which extends the standard system of the AFM, collects the force acting on the cantilever while it is moved by the stepper motor instead of the piezo-system. This is necessary to reach moving distances far above 10 µm, which is the largest operation distance of the piezo element of the *z*-scanner. Tipless cantilevers (ACL-TL from AppNano) with a high spring constant of 65 N/m are being used. The fluid interface is generated in the corresponding liquid cell. The air-water interface is created with an aqueous drop, which is placed onto a hydrophobic surface. The water-air interface uses an air bubble, which is introduced with a syringe in an aqueous environment onto this hydrophobic surface as well. For all measurements, the volume of the drop or bubble is set to a constant. A spherical silica particle of about 30 µm is used as the hydrophilic probe (figure 5). In order to vary the surface properties, i.e. wettability, a second spherical silica particle (40 µm) was coated with Dynasylan® F8261 (Evonik).

To vary the interfacial energy of the fluid, ethanol is added to the liquid phase (from 1 to 15 wt. %). This effects the wetting behavior of the particle. The ethanol content, the surface energy respectively, can be correlated to the measured interaction forces. The surface energy derives from a calculation using the surface tension of water and water-ethanol mixtures, which are taken from the literature [23].

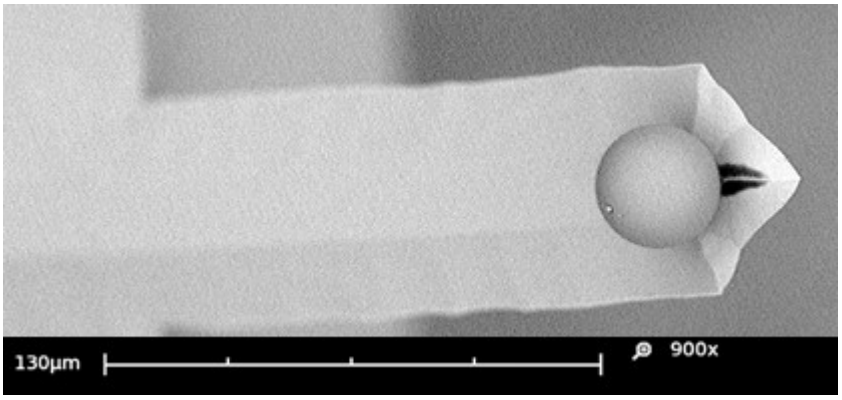

Figure 1: SEM image of a used ACL-TL cantilever with a 30 µm silica colloidal probe

The measuring procedure is presented in figure 2 and will be discussed subsequently.

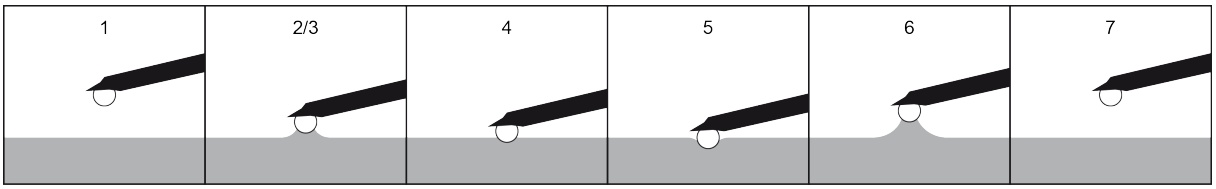

Figure 2: Scheme of the measuring process of a colloidal probe at a cantilever attaching and detaching at the air-air/water interface with the positions: (1) attachment, (2) snap-in and (3) deformation, (4) equilibrium point, (5) deformation and change of direction of movement and (6) deformation until detachment (7); in this case the high stiffness of the cantilever causes a neglectable amount of bending of the cantilever

At first, the cantilever is moved to the interface with a constant velocity of 5 µm/s. The distance between cantilever and interface is large enough that no forces are acting on the particle (position 1). At a certain proximity to the interface, the particle will suddenly come in contact with the interface (position 2), which deflects the cantilever. An attractive capillary force can be measured acting nearly instantaneously on the particle, due to the fast wetting process and the deformation of the interface. This phenomenon is called snap-in. The dynamics of the snap-in were investigated by Chen et al. [24] and McGuiggan et al. [25]. While the cantilever moves further with constant velocity the deformation of the interface is reduced (position 3) until the particle passes a position where the forces acting on the particle are zero (position 4). This equilibrium position is energetically favorable and depends on the surface energies γ_{sl}, γ_{sg} and γ_{lg} at the three-phase-contact-line (TPC). A common method to quantify the surface energies is the method of van Oss et al. [26] via drop shape analysis. A method to determine the dynamic hysteresis of contact angles on a single particle via AFM is described by Ecke et al. [10]. In this study the dynamic contact angles are calculated from the snap-in-distance and the radius of the particle. The moving velocity of the particle influences the dynamic wetting, but the resulting dynamic contact angle is barely influenced by the penetrating velocities of about 5 µm/s, as used in these experiments [16].

Moving the cantilever further in the direction of the drop/bubble will deform the interface in the counter direction. Thus, a repulsive force is acting on the particle against the direction of movement (position 5). At this point, the direction of movement is reversed and the cantilever

is moved away from the interface until the detachment of the particle occurs. After passing through the equilibrium point, once again, the interface is deformed again in the opposite direction (position 6). Finally, at large forces, detachment of the particle from the interface occurs and the force measured becomes zero again (position 7). Figure 3 illustrates a force distance curve obtained from the AFM measurements.

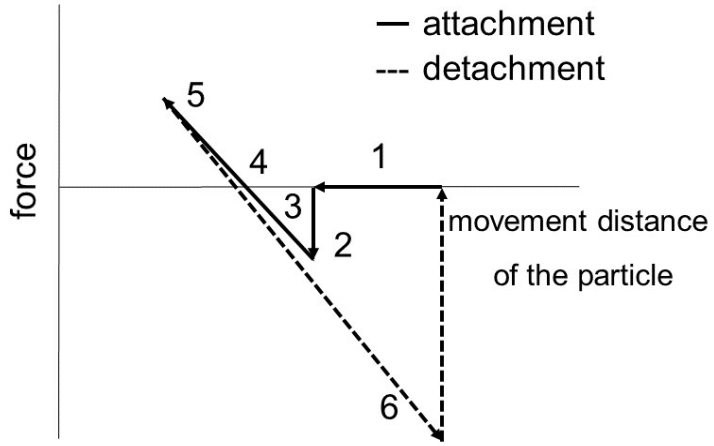

Figure 3: scheme of the force distance curve resulting from AFM measurements

3. Theoretical Approach

For the investigations some assumptions have to be taken into account. The Laplace pressure, which forces the particle out of the drop/bubble is neglectable for the system used. This is because of the small size of the particle compared to the size of the drop/bubble of approximately 1-2 mm. Repulsive viscous forces during the attachment can be neglected as well, due to the low particle velocity applied [27]. Because the drop or bubble is much larger than the particle, a planar interface can be assumed. To investigate wetting and adhesion processes it is convenient to use relatively small particles. Thus, buoyancy and gravitational forces can be neglected as well and thus, only interfacial interactions are considered [9].

The maximum force of detachment, obtained by the analytical model of the acting vertical capillary force, can be found in literature and is shown in the following eq.1 (for detachment from the air/water interface into the water phase) and eq. 2 (for detachment from the water/air interface into the air phase) [13,15,17,18,28,29]. *R* is the radius of the particle, θ the contact angle on the TPC measured through the water phase and γ_{lg} the interfacial surface energy between the liquid and the gaseous phase.

$$F_{\text{A-AW,max}} = -2 \cdot \pi \cdot \gamma_{lg} \cdot R \cdot \cos^2\left(\frac{\theta_{rec}}{2}\right) \quad (1)$$

$$F_{\text{W-WA,max}} = -2 \cdot \pi \cdot \gamma_{lg} \cdot R \cdot \sin^2\left(\frac{\theta_{adv}}{2}\right) \quad (2)$$

To calculate this force, the dynamic contact angle at the TPC has to be known. It is assumed, that during the detachment of a particle from a drop a receding contact angle and during the detachment from a bubble an advancing angle is formed. The formation mechanism and the true nature of the contact angle at the TPC are not widely understood. Some research groups

report, that the TPC of the particle is pinned for the first part of the detachment and the contact angle between the liquid and the surface is changing from a static angle to the dynamic hysteresis contact angle. At the second part of detachment the behavior is reversed and the contact angle remains constant, while the TPC is moving along the particle until detachment [11]. The particle size of the reported system was about 300 µm. Thus, it might not be comparable for smaller particles. It seems obvious, that the contact angle has to change during the detachment process and that the dynamics of this change cannot be measured exactly for the presented detachment process. The apparent contact angles, which are present during this process certainly differ from the constant dynamic contact angle calculated using the snap-in distance of the AFM measurement, as presented by Ecke et al. [10]. Nevertheless, this method is still more appropriate than using static contact angles measured on planar surfaces because one takes the non-planar geometry of the sphere into account. Furthermore, such macroscopic contact angles are difficult to interpret and can be influenced by chemical and physical inhomogeneities on the surface. Therefore, they appear in a wide range [30,31].

Another approach for calculating the force of detachment is a free-energy analysis [11,21]. Figure 4 shows a spherical particle at an air-water (A-AW) interface at the equilibrium point with the radius R, the position angle α, the interfacial areas A_{lg}, A_{sg} and A_{sl} and the penetration distance h, which is the equilibrium distance h_{eq} in this case. The following equations are presented for this A-AW interface. From a thermodynamically point of view, it is well known that the free-energy of a system has to be minimized to reach a steady state. The change of the Gibbs free energy can be assigned with respect to each position of the particle at the interface described by the angle α, while the contact angle remains theoretically constant. This is plausible by the Young equation, where the surface energies are strictly connected to the surface energies which are not changed during the approach or detachment.

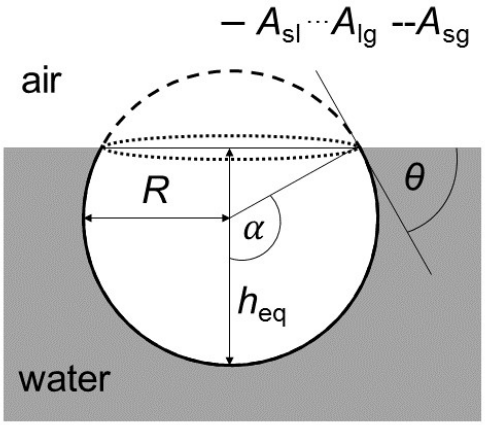

Figure 4: scheme of a particle at an air-water interface located in equilibrium position

The energies W_{sl}, W_{sg}, and W_{lg} between each bulk phases result from the geometry of the sphere and the associated interfacial energies:

$$W_{sl} = 2\pi R^2 \cdot \gamma_{sl}(1-\cos\alpha) \tag{3}$$

$$W_{sg} = 2\pi R^2 \cdot \gamma_{sg}(1+\cos\alpha) \tag{4}$$

$$W_{lg} = \pi R^2 \cdot \gamma_{lg} \sin^2\alpha \tag{5}$$

$$h(\alpha) = R(1-\cos\alpha) \tag{6}$$

The free Gibbs-energy can be calculated as the sum of these energies with the condition that the interfaces between solid/gas and solid/liquid are summarized while the liquid/gas interface is defined as an interface, which will be reduced and has to be subtracted.

$$\sum W_i = W_{Gibbs} = W_{sl} - W_{lg} + W_{sg} \tag{7}$$

The force, which is needed to change the vertical position of the particle within the interface, can then be calculated by:

$$-F = \frac{dW_{Gibbs}}{dh} = -2\pi R\left(\gamma_{lg}\left(1-\frac{h}{R}\right) - \gamma_{sl} + \gamma_{sg}\right) \tag{8}$$

To simplify equation 8, a connection to the Young-equation (eq. 9) is inserted. By this the contact angle is solely considered as a relationship of the three different surface energies as defined by Young [32]. Thus, it is not implicitly comparable with a geometric orientation of the TPC for any other vertical position but the equilibrium position.

$$\cos\theta = \frac{\gamma_{sg} - \gamma_{sl}}{\gamma_{lg}} \tag{9}$$

Finally the linear force-distance trend is:

$$-F = \frac{dW_{Gibbs}}{dh} = -2\pi R\gamma_{lg}\left(1-\frac{h}{R}+\cos\theta\right) = -2\pi R\gamma_{lg}\left(\cos\alpha+\cos\theta\right) \tag{10}$$

The two presented calculation models, the vertical capillary force model (eq. 1) and the Gibbs free-energy analysis (eq. 10) lead to different shapes of the forces-distance curves during detachment and thus, different values of maximum forces needed to completely remove the particle from the equilibrium position, as presented in figure 5. The Gibbs free-energy approach leads to a linear function of the force and with an absolute maximum value located at h = 0 µm. This is the distance, when the particle is barely in contact with the interface. The value of maximum force from the Gibbs free energy approach is much higher (12 µN) than the force obtained from the capillary model (6 µN). Similar values are only obtained, by either model, in the vicinity of the equilibrium position (location of zero force).

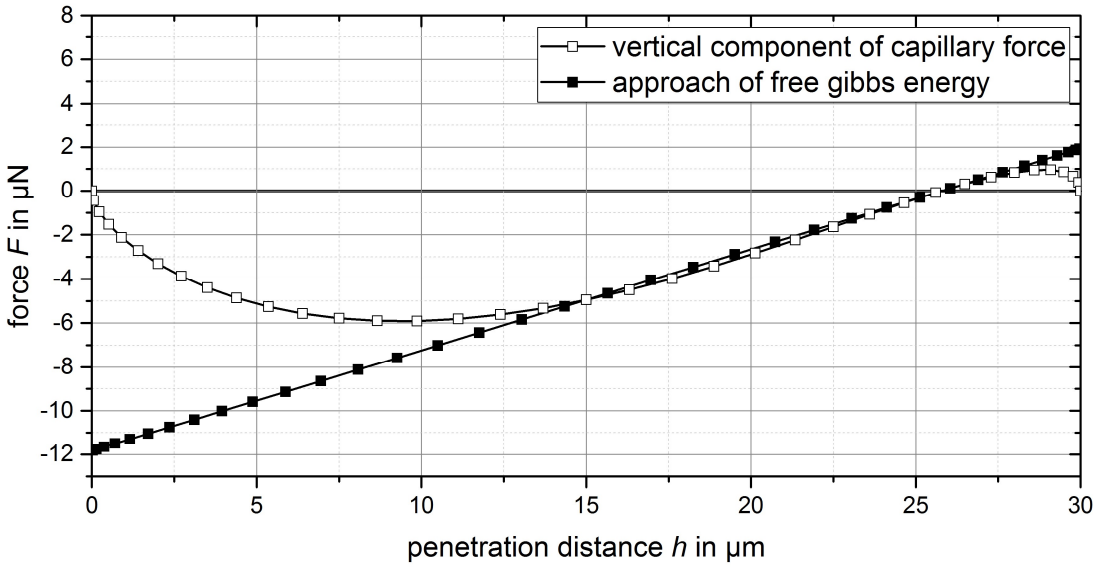

Figure 5: calculated force trend of the vertical component of capillary force and the force from the approach of Gibbs free energy, model system with a 30 µm sized spherical silica particle going through an air-air/water interface (interfacial energy of 0,0727 N/m), with an advancing contact angle of 44° calculated from the snap-in-distance while this particle attaches a bubble

The large forces obtained using the Gibbs free-energy approach derive from the fact that the model (eq. 11) only regards the particle movement through the interface. A second effect, which cannot be neglected for the calculation is the deformation of the interface itself.

This paper will show the difference of the classical calculation models of the detachment force of particles from interfaces and provide a simple analytical model, which is based on energetic considerations, in order to calculate detachment forces while considering the deformation of the interface.

Extended spring model

The total energy of adhesion is the difference of the Gibbs free energies between the state, where the particle is being situated at the equilibrium position and when it is completely surrounded by one of the bulk phases (air at the A-AW-system or water at the W-WA system, respectively). It can be calculated discretely by eq. 11 for the system A-AW and eq. 12 for the opposite direction W-WA [8,33].

$$W_{\mathrm{A,A\text{-}AW}} = \pi R^2 \gamma_{\mathrm{lg}} (1+\cos\theta)^2 \qquad \text{system A-AW} \qquad (11)$$

$$W_{\mathrm{A,W\text{-}WA}} = \pi R^2 \gamma_{\mathrm{lg}} (1-\cos\theta)^2 \qquad \text{system W-WA} \qquad (12)$$

The contact angles used in eq. 12 and 13 define the equilibrium position of the particle.

As mentioned before, when calculating the force curve using the Gibbs free-energy approach (figure 5), any deformation of the interface is not considered, but rather the wetting progress on the particle surface. Therefore, the forces obtained follow a linear trend with respect to the vertical distance. Due to that fact, an effective spring constant can be matched to model this behavior. The slope of the force curve amounts to $2\pi\gamma_{\mathrm{lg}}$. Furthermore, it is reported in the literature, that the deformation of interfaces follows a linear function as well and that an effective spring constant k_{i} for the interface can be assigned [27,34–38]. Taking this into account, we consider a black box of deformation, where the spring constant is not exactly

known for the interface. It depends on various parameters like drop size, particle size and interfacial tension. When expecting a constant force acting during both micro processes, deformation or wetting, a serial connection of two modeled springs can be assumed. The spring constant of the cantilever is much higher compared to both of the single spring constants Therefore its influence on the overall spring constant can be neglected. Calculating the total spring constant k_{tot} of the system gives:

$$\frac{1}{k_{tot}} = \frac{1}{2\pi\gamma_{lg}} + \frac{1}{k_i} \tag{13}$$

Combining the linear force-distance curve with the total deflection of the system of springs yields to:

$$F = k_{tot} \cdot s = \frac{1}{\frac{1}{2\pi\gamma_{lg}} + \frac{1}{k_i}} \cdot s \tag{14}$$

With eq. 14 the force trend in dependence of the total deflection *s* of the spring system is given, which leads to the maximum force F_{max}, is the only unknown parameter. Therefore, an integration of eq. 14 over the maximum distance s_{max} is necessary and gives a value of the energy, which is stored in the spring system.

$$W_{ges} = \int_0^{s_{max}} F\,ds = \frac{1}{2}\frac{1}{\frac{1}{2\pi\gamma_{lg}} + \frac{1}{k_i}} \cdot s_{max}^2 \tag{15}$$

The assumption is made, that the maximum value for the energy, which can be stored in the spring system, is equal to the total energy of adhesion. If this value is reached, the particle will definitely detach from the interface. The spring of interfacial deformation can store more energy than the spring of wetting, due to its lower spring constant assuming equal acting forces on both springs. Thus, the required distance for complete detachment is enlarged. The total deflection s_{max} can be calculated by the following equation:

$$W_{ges} = \frac{1}{2}\frac{1}{\frac{1}{2\pi\gamma_{lg}} + \frac{1}{k_i}} \cdot s_{max}^2 = W_{adh} = \pi\,\gamma_{lg} R^2 (1+\cos\theta)^2 \tag{16}$$

$$s_{max} = \sqrt{\frac{2\pi\gamma_{lg}}{k_i} + 1} \cdot R \cdot (1+\cos\theta) \tag{17}$$

Combining the maximum distance s_{max} with eq. 14 gives the maximum detachment force of the particle:

$$F_{max} = \sqrt{\frac{2\pi\gamma_{lg}}{k_i} + 1} \cdot R \cdot (1+\cos\theta) \cdot \frac{1}{\frac{1}{2\pi\gamma_{lg}} + \frac{1}{k_i}} \tag{18}$$

In the opposite direction when a particle detaches from a gas bubble, a sign has to be turned in the term of the energy of adhesion and the force can be calculated with eq. 14.

$$F_{max} = \sqrt{\frac{2\pi\gamma_{lg}}{k_i} + 1} \cdot R \cdot (1 - \cos\theta) \cdot \frac{1}{\frac{1}{2\pi\gamma_{lg}} + \frac{1}{k_i}} \tag{19}$$

4. Results and discussion

Figure 6 shows the force-distance-curve for a 30 µm sized hydrophilic silica particle, which is attached and detached at the air/water interface. A certain deviation from the expected linear force curve is visible during the end of the detachment process. It is not completely clear, which micro process causes this deviation. A possible reason could be the strong deformation of the interface and a transition from interface bending to an elongation because of the increased length of capillary bridge. In this case the assumption of the linear spring behavior of the interface in no longer valid.

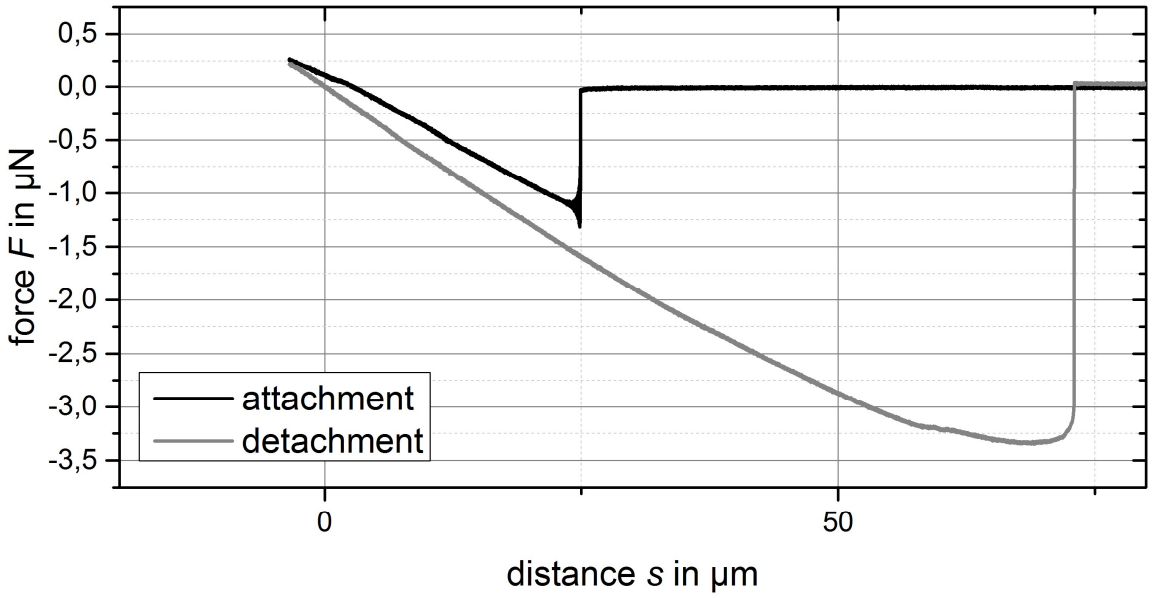

Figure 6: measured force distance curve with a 30 µm hydrophilic silica particle, which is moved in a water drop; the maximum force acting on the particle during detachment is 3,3 µN

Comparing the distance *s*, which the particle needs to detach completely from the interface, to the particle geometry itself, it is obvious that a significant deformation of the interface occurs. With this it can be stated, that the detachment process must be crucially influenced by the deformation of the interface. The AFM measurements provide values for maximum forces of detachment of the single particles from a liquid interface. In figure 7 (left) a comparison of the measured forces with those values obtained from the extended spring model (eq. 14) is presented. For this measurement the hydrophilic particle is detached from a water drop without ethanol. There is a good agreement between the slopes of the measured and modelled force curves. For the interfacial spring constant k_i the surface energy γ_{lg} of 0,0727 N/m is assumed [21,34,35]. The vertical dotted line illustrates the calculated distance, which has to be overcome in order to completely detach the particle from the interface. The total distance calculated by eq. 17 is in the range of the measured one. Calculated (hatched area in figure 7, left) and measured (grey area in figure 7, left) values of the detachment energies are quite equal. The calculated force follows the linear function, while the slope of the measured force decreases at the detachment point and leads to the small difference between measured and calculated force values. The method to calculate the distance of detachment is shown in figure 7 (right) as well. Here the calculated energies from eq. 6 and 17 are plotted and additionally,

the total energy of adhesion for the particle, gained by integral energy analysis (eq. 11) is displayed. The intercept point, where the total energy curve of the spring system reaches the value of the total energy of adhesion, provides the detachment distance.

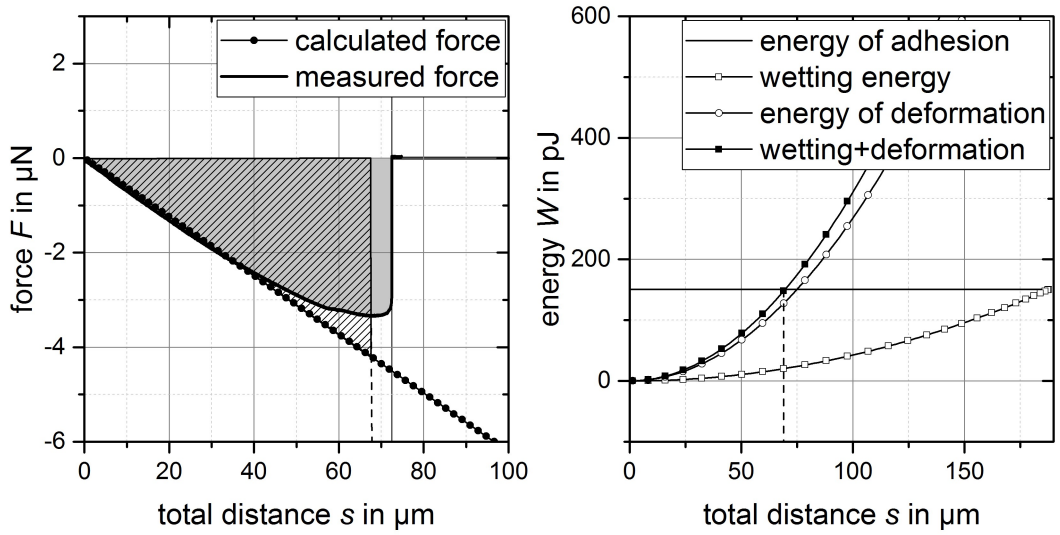

Figure 7: left: comparison of the measured force with the force calculated with aid of the extended spring model, right: determination of the total distance via energy argument; detachment of a 30 µm hydrophilic silica particle from a water drop, a receding contact angle of 44° and an assumed interfacial spring constant of 0,072 N/m; the calculation fits the measurement

Applying the spring model to other systems than the previously presented ideal water-air systems yields to larger differences between the detachment forces. In figure 8 the measured and modelled detachment of the hydrophobic particle from an aqueous drop is illustrated. The effective spring constant of the interfacial deformation in this case should amount a value of $0{,}6\,\gamma_{lg}$ fitting the measured slope.

The assumption of a fixed deformation spring constant in the measured systems and the contact angles calculated from the snap-in-distance cannot be assumed here. These two values have the main influence to the accuracy of the fit:

- The spring constants of drops and bubbles are neither equal nor can be assumed as the value of the exact interfacial surface energy. During the measurements with bubbles and drops the spring constants of interfacial deformation appears in a range of 0,5 to 1,4 γ_{lg}. This value determines the slope of the detachment force and has to be measured for each system.
- The contact angle which is used to calculate the energetic situation of the particle and is constant at any state of detachment in this model. The real behavior of the contact angle in correlation with the deformation of the interface cannot be measured and is still unknown. For this model the contact angle is required to determine the theoretic total distance until the particle leaves the interface.

A possible reason for the correlation of the detachment of a hydrophilic particle from a drop could be the high energy of adhesion. The particle attaches deep into the drop due to the distinctive wettability. Therefore, the accuracy of the energy measurement of particles with small contact angles is quite better compared with larger ones.

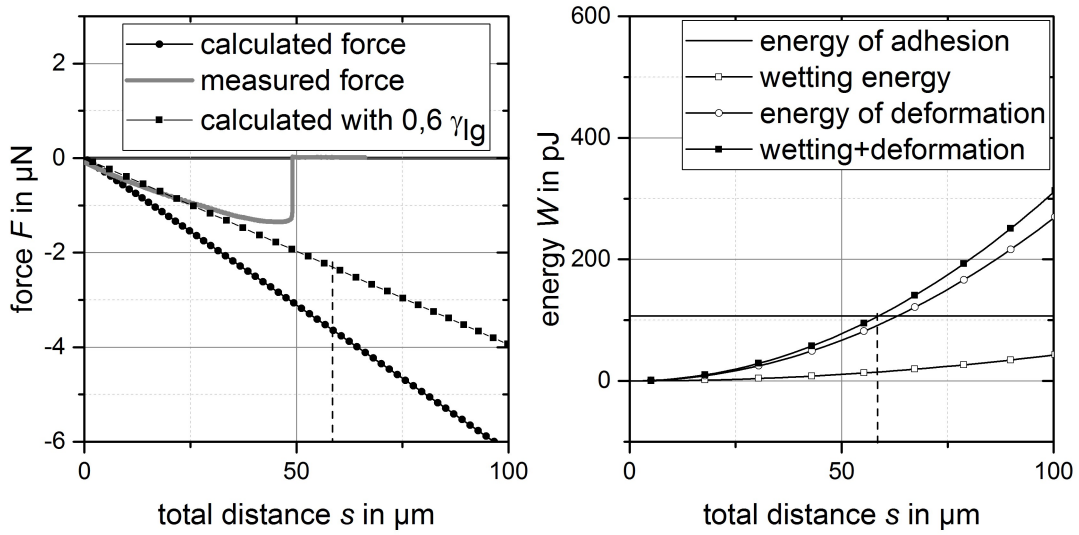

Figure 8: left: comparison of the measured force with the force calculated by the extended spring model and the calculated force with 0,6 γ_{lg} as spring constant of interfacial deformation, right: determination of the total distance via energy argument; detachment of a 40 µm hydrophobic silica particle from a water drop, a receding contact angle of 85° and an assumed interfacial spring constant of 0,072 N/m; the measurement does not fit the calculation

Nevertheless, in the case of a detachment of a hydrophilic particle from a drop the calculated forces with the assumption $k_i = \gamma_{lg}$ and the receding contact angle of 44° fits better to the measured ones compared to the classic calculation model of vertical capillary force as presented in figure 9. The detachment force is a function of the chemical composition of the interface, which changes with the ethanol concentration in the liquid phase. The ethanol is used to reduce the interfacial energy between air and aqueous phase [23] as well as the forming contact angle. Thus, the forces measured decrease slightly with increasing ethanol concentration, as presented in figure 9 as well.

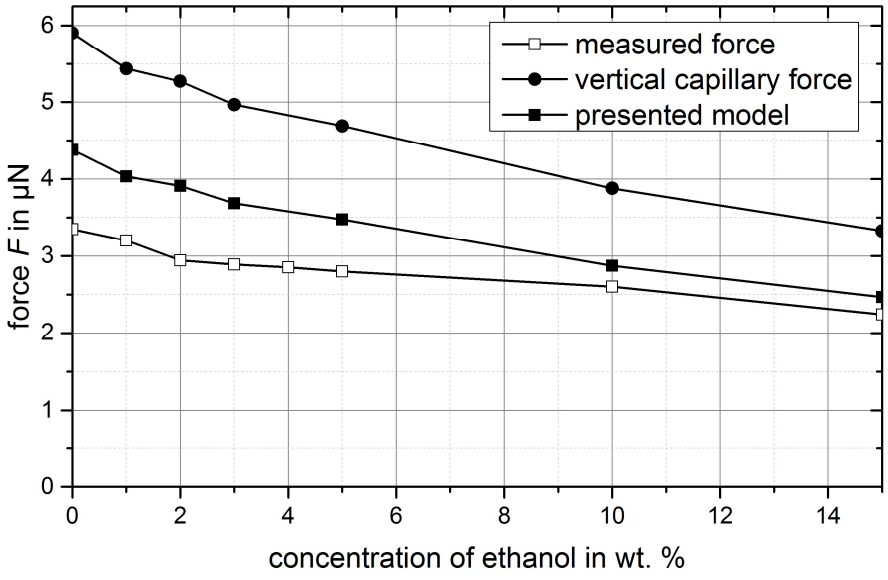

Figure 9: comparison of measured and calculated forces in correlation with the concentration of ethanol in a water droplet; the forces calculated with the receding contact angle measured via AFM for a hydrophilic particle with a diameter of 30 µm

5. Conclusion

The paper presents an alternative model for calculating the force needed to pull a particle out of a droplet. The main assumption of the model is a theoretic spring system of two springs which deflect during the detachment process. The springs represent the deformation of the interface and the wetting of the particle. The real values of the interfacial spring constant and the change of the contact angle during the detachment are unknown and need to be assumed. Nevertheless, this work gives a contribution to the understanding of the detachment of micro particles from deformable liquid interfaces and shows the deviation of measured and calculated forces from the commonly used model of vertical capillary force in this case.

Acknowledgement

The authors gratefully thank the German Research Foundation (DFG) for supporting the Collaborative Research Center CRC 920, subproject B04.

REFERENCES

[1] B. Pyke, D. Fornasiero, J. Ralston, Bubble particle heterocoagulation under turbulent conditions, J Colloid Interface Sci 265 (2003) 141–151.
[2] J. Ralston, D. Fornasiero, R. Hayes, Bubble–particle attachment and detachment in flotation, International Journal of Mineral Processing 56 (1999) 133–164.
[3] F. Heuzeroth, J. Fritzsche, U.A. Peuker, Wetting and its influence on the filtration ability of ceramic foam filters, Particuology 18 (2015) 50–57.
[4] L. Ditscherlein, J. Fritzsche, U.A. Peuker, Study of nanobubbles on hydrophilic and hydrophobic alumina surfaces 497 (2016) 242–250.
[5] J. Fritzsche, U.A. Peuker, Wetting and Adhesive Forces on Rough Surfaces – An Experimental and Theoretical Study, Procedia Engineering 102 (2015) 45–53.
[6] M. Rudolph, U.A. Peuker, Hydrophobicity of Minerals Determined by Atomic Force Microscopy - A Tool for Flotation Research, Chemie Ingenieur Technik 86 (2014) 865–873.
[7] M. Rudolph, U.A. Peuker, Mapping hydrophobicity combining AFM and Raman spectroscopy, Minerals Engineering 66-68 (2014) 181–190.
[8] B.P. Binks, Particles as surfactants—similarities and differences, Current Opinion in Colloid & Interface Science 7 (2002) 21–41.
[9] A. Maestro, E. Guzmán, F. Ortega, R.G. Rubio, Contact angle of micro- and nanoparticles at fluid interfaces, Current Opinion in Colloid & Interface Science 19 (2014) 355–367.
[10] S. Ecke, M. Preuss, H.-J. Butt, Microsphere tensiometry to measure advancing and receding contact angles on individual particles, Journal of Adhesion Science and Technology 13 (1999) 1181–1191.
[11] O. Pitois, X. Chateau, Small Particle at a Fluid Interface: Effect of Contact Angle Hysteresis on Force and Work of Detachment, Langmuir 18 (2002) 9751–9756.
[12] G.E. Yakubov, O.I. Vinogradova, H.-J. Butt, Contact angles on hydrophobic microparticles at water–air and water–hexadecane interfaces, Journal of Adhesion Science and Technology 14 (2000) 1783–1799.
[13] J. Ally, M. Kappl, H.-J. Butt, A. Amirfazli, Detachment force of particles from air-liquid interfaces of films and bubbles, Langmuir 26 (2010) 18135–18143.
[14] G. Gillies, K. Büscher, M. Preuss, M. Kappl, H.-J. Butt, K. Graf, Contact angles and wetting behaviour of single micron-sized particles, J. Phys.: Condens. Matter 17 (2005) S445.
[15] D.J. Johnson, N.J. Miles, N. Hilal, Quantification of particle-bubble interactions using atomic force microscopy: A review, Adv Colloid Interface Sci 127 (2006) 67–81.

[16] A.V. Nguyen, J. Nalaskowski, J.D. Miller, The dynamic nature of contact angles as measured by atomic force microscopy, J Colloid Interface Sci 262 (2003) 303–306.
[17] M. Preuss, H.-J. Butt, Direct measurement of forces between particles and bubbles, International Journal of Mineral Processing 56 (1999) 99–115.
[18] Preuss, M., et al., Preuss, Butt, Measuring the Contact Angle of Individual Colloidal Particles, J Colloid Interface Sci 208 (1998) 468–477.
[19] S. Ren, J. Masliyah, Z. Xu, Studying bitumen–bubble interactions using atomic force microscopy 444 (2014) 165–172.
[20] J. Ally, M. Kappl, H.-J. Butt, Adhesion of particles with sharp edges to air-liquid interfaces, Langmuir 28 (2012) 11042–11047.
[21] R. Ettelaie, S.V. Lishchuk, Detachment force of particles from fluid droplets, Soft Matter 11 (2015) 4251–4265.
[22] G.B. Davies, T. Krüger, P.V. Coveney, J. Harting, Detachment energies of spheroidal particles from fluid-fluid interfaces, J Chem Phys 141 (2014) 154902.
[23] G. Vazquez, E. Alvarez, J.M. Navaza, Surface Tension of Alcohol Water + Water from 20 to 50 Grad Celsius, J. Chem. Eng. Data 40 (1995) 611–614.
[24] L. Chen, L.-O. Heim, D.S. Golovko, E. Bonaccurso, Snap-in dynamics of single particles to water drops, Appl. Phys. Lett. 101 (2012) 031601.
[25] P.M. McGuiggan, D.A. Grave, J.S. Wallace, S. Cheng, A. Prosperetti, M.O. Robbins, Dynamics of a disturbed sessile drop measured by atomic force microscopy (AFM), Langmuir 27 (2011) 11966–11972.
[26] C.J. van Oss, M.K. Chaudhury, R.J. Good, Interfacial Lifshitz-van der Waals and polar interactions in macroscopic systems, Chem. Rev. 88 (1988) 927–941.
[27] A.V. Nguyen, G.M. Evans, J. Nalaskowski, J.D. Miller, Hydrodynamic interaction between an air bubble and a particle: atomic force microscopy measurements, Experimental Thermal and Fluid Science 28 (2004) 387–394.
[28] A. Scheludko, B.V. Toshev, D.T. Bojadjiev, Attachment of particles to a liquid surface (capillary theory of flotation), J. Chem. Soc., Faraday Trans. 1: 72 (1976) 2815.
[29] F. Omota, A.C. Dimian, A. Bliek, Adhesion of solid particles to gas bubbles. Part 1: Modelling, Chemical Engineering Science 61 (2006) 823–834.
[30] S. Cappelli, Q. Xie, J. Harting, de Jong, A M, Prins, M W J, Dynamic wetting: status and prospective of single particle based experiments and simulations, New biotechnology 32 (2015) 420–432.
[31] L. Gao, T.J. McCarthy, Contact angle hysteresis explained, Langmuir 22 (2006) 6234–6237.
[32] T. Young, An Essay on the Cohesion of Fluids, Philosophical Transactions of the Royal Society of London 95 (1805) 65–87.
[33] A.F. Koretsky, P.M. Kruglyakov, Emulsifying effects of solid particles and the energetics of putting them at the water–oil interface, Izv. Sib. Otd. Akad. Nauk. SSSR Ser. Khim. Nauk 2 (1971) 139–141.
[34] P. Attard, S.J. Miklavcic, Effective Spring Constant of Bubbles and Droplets, Langmuir 17 (2001) 8217–8223.
[35] P. Attard, S.J. Miklavcic, Effective Spring Description of a Bubble or a Droplet Interacting with a Particle, J Colloid Interface Sci 247 (2002) 255–257.
[36] M.L. Fielden, R.A. Hayes, J. Ralston, Surface and Capillary Forces Affecting Air Bubble−Particle Interactions in Aqueous Electrolyte, Langmuir 12 (1996) 3721–3727.
[37] M. Preuss, H.-J. Butt, Direct Measurement of Particle−Bubble Interactions in Aqueous Electrolyte: Dependence on Surfactant, Langmuir 14 (1998) 3164–3174.
[38] Dupré de Baubigny, Julien, M. Benzaquen, L. Fabié, M. Delmas, J.-P. Aimé, M. Legros, T. Ondarçuhu, Shape and Effective Spring Constant of Liquid Interfaces Probed at the Nanometer Scale: Finite Size Effects, Langmuir 31 (2015) 9790–9798.